OFFICE OF NAVAL RESEARCH

Grant N00014-89-J-1261

R&T Code 4131038

ONR Technical Report
#31

Phosphatidylcholine Monolayer Formation at a Liquid:Liquid Interface as Monitored by the Dynamic Surface Tension

by

R. A. Walker and G. L. Richmond

Langmuir, submitted

Department of Chemistry
1253 University of Oregon
Eugene, OR 97403

June 1998

REPORT DOCUMENTATION PAGE

Form Approved
OMB No. 0704-0188

1. AGENCY USE ONLY (Leave Blank)	2. REPORT DATE	3. REPORT TYPE AND DATES COVERED
	30 May 1998	Technical 3/1/97-5/31/98

4. TITLE AND SUBTITLE
Phosphatidylcholine Monolayer Formation at a Liquid:Liquid Interface as Monitored by the Dynamic Surface Tension

5. FUNDING NUMBERS
N00014-89-J-1261

6. AUTHOR(S)
R. A. Walker and G. L. Richmond

7. PERFORMING ORGANIZATION NAME(S) AND ADDRESS(ES)

Dept of Chemistry
University of Oregon
Eugene, OR 97403

8. PERFORMING ORGANIZATION REPORT NUMBER

ONR Technical Report
#31

9. SPONSORING/MONITORING AGENCY NAME(S) AND ADDRESS(ES)

Dr. Peter Schmidt
Office of Naval
Research Physical
Science and Technology, ONR 331
800 North Quincy Street
Arlington, VA 22217-5000

10. SPONSORING/MONITORING AGENCY

11. SUPPLEMENTARY NOTES

Langmuir, submitted

12A. DISTRIBUTION / AVAILABILITY STATEMENT

Approved for public release: distribution unlimited

12B. DISTRIBUTION CODE

13. ABSTRACT (Maximum 200 words)

Please see attached
abstract

14. SUBJECT TERMS
Dynamic Surface Tension Phospholipid Monolayer Formation at a Planar Aqueous: CCl4 Interface

15. NUMBER OF PAGES
48

16. PRICE CODE

17. SECURITY CLASSIFICATION OF REPORT	18. SECURITY CLASSIFICATION OF THIS PAGE	19. SECURITY CLASSIFICATION OF ABSTRACT	20. LIMITATION OF ABSTRACT
Unclassified	Unclassified	Unclassified	

Phosphatidylcholine Monolayer Formation at a Liquid:Liquid Interface as Monitored by the Dynamic Surface Tension

Robert A. Walker and Geraldine L. Richmond*

University of Oregon, Eugene, OR 97403

Abstract: Dynamic surface tension experiments have monitored the rate of phospholipid monolayer formation at a planar aqueous:CCl_4 interface from a solution of phosphatidylcholine (PC) vesicles. The rates at which monolayers form show that monolayer formation is a barrier controlled rather than a diffusion controlled process. At sufficiently low bulk PC concentrations, monolayer formation kinetics are first order in aqueous PC concentration. The kinetics can be described by a rupture mechanism which postulates that vesicles disintegrate at the aqueous:CCl_4 boundary allowing all of the monomers to adsorb to the interface. When coupled to an appropriate two dimensional equation of state this mechanism quantitatively models the observed dynamic surface tension data. Solutions of vesicles in their liquid crystalline phase form tightly packed monolayers at concentrations above ~2 μMolar, while solutions of gel phase vesicles form expanded monolayers regardless of bulk PC concentration. From the Arrhenius behavior of the dynamic surface tension data, we find that the barrier to monolayer formation is larger for solutions of liquid crystalline vesicles than for solutions of gel state vesicles. These phenomena - the extent of monolayer formation and E_a for monolayer formation - support a model which describes monolayer formation as a thermodynamically driven transformation from monomers within a bilayer to monomers adsorbed at the aqueous:CCl_4 interface.

I. Introduction

A distinguishing characteristic of long chain phospholipids is their ability to form vesicles in aqueous solutions. These uni or multilamellar bilayer structures serve as the simplest biomimetic models of biological cell systems and considerable effort has gone into studying how bilayer composition affects physical properties such as permeability,[1,2] structural disorder,[3-6] and chemical stability.[7] Phospholipid vesicles have also found application as vehicles in drug delivery systems.[8,9] Given the exquisite control researchers can exercise over vesicle size characteristics,[10-12] phospholipid vesicles appear to provide a very attractive means of transporting pharmaceuticals *in vitro* to specific areas within the body. Essential to their role as biological membrane models and microscopic transport systems is the issue of vesicle structural integrity. For almost two decades researchers have known that solutions of phospholipid vesicles form monolayers of phospholipid monomers at air:aqueous interfaces.[13,14] Efforts to structurally modify vesicles by incorporating membrane proteins and/or cholesterol have led to formation of binary monolayer systems at a variety of interfaces.[15-17] Related work has examined intervesicle exchange of phospholipid monomers.[18-24] These phenomena - monolayer formation and monomer exchange - necessarily require that vesicles themselves be dynamic structures rather than rigid, static bodies.[25] The goal of this work lies in examining phospholipid monolayer formation at a planar liquid:liquid interface where one of the fluid phases is an aqueous solution of phosphatidylcholine (PC) vesicles. With the Wilhelmy plate method we monitor the rate of monolayer formation by measuring the dynamic surface tension of an aqueous:carbon tetrachloride interface. We show that monolayer formation kinetics depend not only on aqueous PC concentration but also on vesicle bilayer phase. We also calculate activation energies for the monolayer formation process and find that vesicles in the liquid crystalline phase must surmount a larger barrier to form monolayers than gel phase vesicles.

In 1978 Verger and coworkers demonstrated that monolayers of phospholipid monomers will form from aqueous solutions of phospholipid vesicles.[13] Shortly thereafter Schindler examined monolayers formed in this fashion at the aqueous:air interface and found that monomers exchange freely with an underlying layer of phospholipid vesicles.[14] These studies concluded that the surface layer possesses an appreciably higher concentration of vesicles than the bulk solution and that in the limit of an infinitely dilute monolayer, vesicles probably disintegrate completely on contact with the interface.[14] MacDonald and Simon examined the relationship between lipid bilayer phase and the rate of monolayer formation.[26] Working with solutions of DMPC vesicles above the gel-liquid crystalline transition temperature ($T_c = 23^\circ$ C), the authors found that aqueous solutions of DMPC vesicles rapidly equilibrated with the air:aqueous interface, forming monolayers with a surface pressure of 49 mN/m. In contrast aqueous solutions of DMPC vesicles below T_c required days to equilibrate and even then the monolayer formed was considerably more expanded than that formed from vesicles above T_c.

Similar effects have been observed in rates of intervesicle monomer exchange. McLean and Phillips noted that the rate of DMPC monomer exchange between small, unilamellar DMPC vesicles exhibited an abrupt, discontinuous rise in the vicinity of the lipid bilayer gel-liquid crystalline transition temperature.[22] Additional studies reported that monomer exchange between vesicles constituted a first order process[20] and the rate of transfer decreased exponentially with increasing acyl chain length.[27] Two different mechanisms arose to explain these results: a) transfer of monomers through solution and b) monomer transfer via vesicle collision. Yang and Huestis demonstrated how each mechanism provided a consistent explanation of observed transfer phenomena under different conditions.[18] Through-solution exchange adequately described data for more hydrophilic lipids while the collision mechanism worked well for more hydrophobic species. Potentially, both mechanisms could play important roles during formation of a

monolayer from a solution of PC vesicles. If monolayer formation proceeded primarily by means of through-solution transport of monomers, then we might expect monolayers to form quite slowly as monomers adsorbed to the interface one by one. However, a mechanism which required a collision between vesicles and the interface would favor the vesicle disintegration picture inferred in earlier studies[14] and allow monolayers to form more rapidly.

The experiments described in this paper address the way in which aqueous solutions of phosphatidylcholine vesicles form monolayers of monomers adsorbed to a planar aqueous:carbon tetrachloride interface (Figure 1). Specifically, we find that the rate of monolayer formation depends on bulk PC concentration as well as temperature. Dynamic surface tension experiments show several different regimes of monolayer formation kinetics. At bulk PC concentrations below ~2μMolar and at temperatures above T_c, the surface tension exhibits single exponential decay behavior, slowly approaching an asymptotic limit characteristic of the bulk PC concentration and the system's temperature. In the high concentration limit above T_c, the surface tension diminishes rapidly in a fashion not readily characterized by a simple functional form. When the experimental temperature lies below a system's T_c, monolayer formation happens very slowly, regardless of bulk PC concentration. We show how a simple kinetic model coupled to an appropriate two dimensional equation of state explains all of the observed phenomena. The mechanism requires that PC monolayers form from complete rupture of vesicles at the interface. A mechanism which postulates that monomers adsorb individually does not accurately describe the observed kinetics. From studying the temperature dependence of the monolayer formation kinetics, we calculate activation energies for the monolayer formation process and find fundamentally different behavior depending on whether aqueous phase vesicles are in their gel or liquid crystalline phase. Our results share similarities with data

from intervesicle monomer exchange studies, and we can relate our findings to physical properties of the vesicle bilayer structure.

II. Experimental

A. Sample Preparation

The phosphatidylcholines used in this work belong to a family of saturated, symmetric, diacyl phosphatidylcholines (Figure 2a) with chains ranging in length from C_{12} (dilauroyl-sn-phosphatidylcholine, DLPC) to C_{18} (distearoyl-sn-phosphatidylcholine, DSPC) in increments of two methylene units (C_{14} = dimyristoyl-sn-phosphatidylcholine, DMPC; C_{16} = dipalmitoyl-sn-phosphatidylcholine, DPPC). In aqueous solution these phosphatidylcholines spontaneously aggregate to form bilayer sheets. Upon sonication, these sheets reorganize to form uni or multilamellar bilayer vesicles.[12] The thermodynamic phase of these bilayer vesicles depends on the temperature of the solution: at low temperatures the bilayer interiors are frozen in a gel phase (P_β) while at higher temperatures, the chains melt and assume a more fluid, disordered liquid crystalline phase (L_α). (Figure 2b) Phase transition temperatures (T_c) vary with PC chain length (Table 1).

The solubility of PC monomers in solution remains exceedingly small during all of the experiments described below. Using fluorescent tagged PC monomers, Nichols measured the bilayer:free monomer partition coefficients for analogs of DMPC, DPPC and DSPC and found partitioning into the bilayer to increase sharply with each additional pair of methylene units (~1 x 10^7 for DMPC analog, ~1 x 10^8 for DPPC analog, $\geq 10^9$ for DSPC analog).[21] For our experiments aqueous PC concentration lies between ~0.5 and 10 μMolar, meaning that even at the highest aqueous concentrations, the number of free DLPC monomers in solution represents less than 1% of the number necessary to form a tightly packed monolayer (extrapolating the partition coefficient for DLPC to be 1 x 10^6 bilayer/free monomer).

The four different phosphatidylcholines were purchased as lypholized powders from Avanti Polar Lipids (>99.9% pure) and used as received. The aqueous phase consisted of H_2O (Barnsted Nanopure, 18 MΩ) that had been washed with CCl_4 to remove any small organic contaminants. All aqueous solutions were buffered with a sodium phosphate solution to a pH of 7.0 (10 mMolar in phosphate ion). The purity of carbon tetrachloride (Aldrich, reagent grade or Baker, reagent grade) was confirmed by FTIR and ^1H NMR. Interfacial tension measurements of the neat water:carbon tetrachloride interface produced results in agreement with literature values, [28] indicating an absence of any detectable surface active contaminants in the two solvents.

Phosphatidylcholine stock solutions were prepared by suspending a measured amount of phosphatidylcholine in 5 ml of buffered H_2O and then sonicating the solution above the appropriate phase transition temperature. This procedure created a solution of vesicles ranging in diameter from 60 -150 nm (sample dependent) as determined from dynamic light scattering measurements. Typical concentrations of these stock solutions ranged from 0.5 mMolar to 2.0 mMolar. Phosphatidylcholine sample solutions used in the experiments were prepared by adding a small volume of the stock solution to a volumetric flask containing 25 mL of buffered H_2O. Concentrations of the solutions used in experiments varied between 0.05 μMolar and 50 μMolar. Flasks used for sample solutions were rinsed repeatedly with PC solutions of equivalent concentration in order to eliminate any possible effect of PC adsorption to flask walls.

Solutions prepared from freshly sonicated phosphatidylcholine stock solutions showed higher surface activity than those made from stock solutions which had aged several hours in agreement with the findings of Qiu and MacDonald.[29] After creating a phosphatidylcholine stock solution, we allowed a minimum of 10-12 hours to elapse before preparing sample solutions. Further waiting led to no additional change in PC surface activity. Stock solutions were replaced every 5 days.

B. Interfacial Tension Measurements

Interfacial tension measurements at the water:carbon tetrachloride interface were carried out with a Wilhelmy plate microbalance assembly (KSV Instruments) and a 6 cm diameter glass crystallizing dish. An experiment consisted of first depositing a 20 ml aliquot of CCl_4 into the dish followed by a gentle 25 ml addition of a PC solution. With the interface established, a platinum plate was lowered so that its top edge lay submerged beneath the air:aqueous surface and its bottom edge extended ~1 mm below the nominal aqueous:CCl_4 interface (Fig 3a). This experimental approach had the disadvantage of missing the initial moments (~45-60 sec) of monolayer formation. However, monolayers typically required many hours to equilibrate and for sufficiently low PC concentrations, the interfacial tension at the start of data collection differed from the tension of the neat aqueous:CCl_4 interface by less than 1 mN/m. This technique of premixing the PC solutions reduced the effects of convection and anomalous concentration gradients in the aqueous phase. We also conducted a series of experiments in which we first established a neat interface and then made a small volume addition of the high concentration PC stock solution, raising the aqueous concentration to the desired value. [30-32] This method allowed us to ascertain the tension of the neat interface thus ensuring interfacial purity. However, this analytical convenience came at the expense of a uniformly mixed aqueous phase following the small volume stock solution addition. In the low concentration limit data from both techniques agreed quite well. At higher bulk PC concentrations the small volume addition approach led to an initial steep drop in tension followed by a more gradual approach to an asymptotic limit.

Most experiments were carried out under ambient conditions (21-23° C). Thermally controlled experiments designed to investigate the effect of temperature on monolayer formation kinetics involved attaching a water jacket around the crystallizing dish. A circulating bath allowed for temperature control to ± 1° C. Although CCl_4 boils at ~70° C, the aqueous layer effectively reduced the boiling point to ~50° C imposing an

upper limit to the accessible temperature range. Temperature dependent dynamic surface tension measurements were carried out in a window between 5° C and 45° C.

As the PC monolayer formed at the aqueous:CCl_4 interface, the surface tension (γ) decreased, slowly approaching an equilibrium value. Terminal $\gamma(t)$ readings were recorded when the rate of change of $\gamma(t)$ fell to less than 2% of $\gamma_0 - \gamma(t)$ per hour. (γ_0 represents for the tension of the neat aqueous:CCl_4 interface, 44.5 mN/m.[28]) Values of equilibrium surface tension were converted to surface pressures ($\Pi_e = \gamma_0 - \gamma_e$) and plotted versus bulk PC concentration in order to map out adsorption isotherms and measure the extent of monolayer formation. Representative isotherms for DLPC and DSPC at room temperature appear in Figure 3b. Terminal surface pressures of DLPC monolayers adsorbed to the water:carbon tetrachloride interface agree reasonably well with reported results of phosphatidylcholine monolayers adsorbed to alternative aqueous:organic interfaces.[33-36] Analyzing the isotherm data by means of the Gibbs equation shows that aqueous solutions of DLPC vesicles at room temperature form tightly packed monolayers with surface concentrations of $1.8 \pm 0.3 \times 10^{14}$ molecules/cm^2 (55 Å^2/molecule).[30,31,37] Furthermore, this terminal surface coverage occurs at bulk DLPC concentrations of $\geq 2\mu$Molar. In contrast solutions of DSPC vesicles under ambient conditions form expanded monolayers regardless of bulk concentration. Differences between the two systems can be traced to the lipid bilayer phase dependent behavior of monolayer formation. (Vide infra.)

III. Dynamic Surface Tension Modeling

A. Barrier versus Diffusion Controlled Kinetics

Solutions of phosphatidylcholine vesicles form monolayers of phosphatidylcholine monomers at interfaces.[13-15,26] As our primary objective we seek to understand monolayer formation at the planar boundary formed between an aqueous solution of PC vesicles and an underlying organic phase of carbon tetrachloride. The issue of surfactant adsorption kinetics has received considerable attention for many years.[38-45] In particular a

number of studies have specifically examined adsorption kinetics at liquid:liquid interfaces.[46-50] Adsorption can be described as having two limits: diffusion controlled adsorption and barrier controlled adsorption. Both situations define a subsurface layer as an intermediate region between the surface and the bulk solution.[45,47] In the case of diffusion controlled kinetics, adsorption from the subsurface to the surface occurs quickly and diffusion of surfactants from the bulk to the subsurface layer represents the limiting step in monolayer formation. The rate of monolayer formation obeys traditional laws for mass transport and the subsurface concentration remains depleted (in the absence of desorption). Barrier controlled adsorption refers to a situation in which a barrier exists to transfer of amphiphiles from the subsurface to the surface. In this case the subsurface and the bulk concentrations of amphiphiles are equal and the kinetics of monolayer formation can be characterized by a well chosen rate expression.

To understand PC monolayer formation at the aqueous:CCl_4 interface, we must first determine whether monolayer formation follows diffusion controlled or barrier controlled kinetics. Implicit in this analysis is the assumption that the measured dynamic surface tension can be related to the time dependent surface concentration in a well defined manner. The choice of an appropriate equation of state relating measured surface tension to surface concentration is addressed a subsequent section.

The first physically based model used to describe diffusion controlled kinetics was developed Ward and Tordai.[45] Their approach drew from the well developed theory for heat transfer and expressed adsorption (or surface concentration) in the following form:

$$\Gamma(t) = 2\sqrt{\frac{D}{\pi}}\left(c_o\sqrt{t} - \int_0^{\sqrt{t}} c(0, t-\tau)d\sqrt{\tau}\right) \qquad (1)$$

where

Γ = surface concentration (mole/m^2)

c_o = bulk surfactant concentration (mole/m^3)

D = Diffusion coefficient (m^2/s)

t = time (s)

π = 3.1415. . .

This form of the surface concentration does not possess an analytical solution but it can be simplified depending on whether equilibration of the monolayer occurs quickly or slowly relative to the characteristic diffusion time of the system. [48] Provided that the monolayer remains expanded (low Γ), the surface concentration can be directly related to the measured surface tension. The short time approximation of Eq. 1 states that the surface concentration (and the surface tension) scales as $t^{1/2}$ while the long time approximation predicts that surface tension should scale as $t^{-1/2}$: [48,51]

Short Time Approximation:

$$\gamma(t) \propto \sqrt{\frac{Dt}{\pi}} \tag{2}$$

Long Time Approximation:

$$\gamma(t) \propto \sqrt{\frac{\pi}{4Dt}} \tag{3}$$

where

$\gamma(t)$ = time dependent surface tension (mN/m).

If monolayer formation follows diffusion controlled kinetics, then plotting $\gamma(t)$ against either $t^{1/2}$ or $t^{-1/2}$ should result in a straight line. If monolayer formation results from a barrier controlled process, the time dependent surface concentration (and surface tension) will be determined by an appropriate rate equation.

Figure 4 shows the dynamic surface tension of the aqueous:CCl_4 interface for a 1 μMolar solution of DLPC vesicles. The top two panels plot $\gamma(t)$ versus $t^{-1/2}$ and $t^{1/2}$, respectively (Figures 4a and 4b). If monolayer formation were diffusion controlled in the long time limit, then the tension data in Figure 4a should exhibit linear behavior closer to the origin. Diffusion limited behavior in the short time limit should show $\gamma(t)$ depending linearly on $t^{1/2}$ in Figure 4b. Clearly, $\gamma(t)$ is not linear in either the Figure 4a or 4b. A plot of the surface tension versus time appears in the bottom panel of Figure 4. In general $\gamma(t)$ follows a single exponential decay for bulk PC concentrations ≤ 1 μMolar. At higher concentrations the time dependent surface tension decays in a more complicated fashion. Taken together, the three castings of the dynamic surface tension shown in Figure 4 strongly suggest that PC monolayer formation at an aqueous:CCl_4 interface from a solution of PC vesicles represents a barrier controlled rather than a diffusion controlled process.

Characterizing the time dependent surface tension for a barrier controlled process requires formulating a rate expression for the time dependent surface concentration (n(t)) and relating n(t) to $\gamma(t)$ by means of a 2-dimensional equation of state. In creating a kinetic model we assume that the barrier to monolayer formation arises from either extracting PC monomers from vesicles or complete vesicle rupture at the aqueous:CCl_4 interface. These two mechanisms represent the extraction mechanism and rupture mechanism described below. We also postulate that at low monolayer concentrations vesicles are not surface active, a reasonable assumption given that the hydrophobic acyl chains of the PC monomers lie buried in the vesicle bilayer interior and that the outer surface of the vesicle consists of zwitterionic charged headgroups. At higher monolayer concentrations Coulombic attractions between the headgroups of adsorbed monomers and the charged vesicle shells may lead to higher vesicle concentration at the interface.[14] Finally, we propose that at sufficiently low PC concentrations, the lopsided partitioning of PC monomers into bilayers (vs. free in solution), renders the effect of free monomer

adsorption inconsequential. Based on the partitioning results discussed in the Experimental section, we expect a vanishingly small aqueous phase concentration of free monomers.

B. Kinetic Mechanisms

1. Extraction Mechanism

The monomer extraction model requires that each PC vesicle deposit some fraction of its monomers at the interface one monomer at a time. This mechanism assumes that the vesicles themselves remain intact and that the number of vesicles remaining after the monolayer has equilibrated is approximately equal to the number of vesicles prior to the start of monolayer formation. In order for this condition to be true the total number of PC molecules in aqueous solution must be much greater than the number of molecules to form a tightly packed monolayer at the aqueous:CCl_4 interface. Otherwise, formation of a monolayer will necessarily result in destruction of vesicles. With this model the rate of monomer adsorption at the interface can be described by simple pseudo-zeroth order kinetics:

$$\frac{dn(t)}{dt} = kv_o \tag{4}$$

Here, n(t) represents the time dependent surface concentration, k equals the rate constant for monomer extraction from the vesicle bilayer and v_o reflects the vesicle concentration in the subsurface layer during the monolayer formation process. Because the right hand side of Eq. 4 is a constant for a given temperature and PC concentration, the differential equation is readily integrated to provide a solution for n(t):

$$n(t) = kv_o t \tag{5}$$

At sufficiently low concentrations, the monomer extraction mechanism either limits the equilibrium surface concentration or begins to break down as the vesicles become too small

to remain thermodynamically stable, which, in turn, would lead to vesicle rupture. Complete vesicle decomposition represents the second proposed mechanism of monolayer formation.

2. Rupture Mechanism

The vesicle rupture mechanism involves a PC vesicle approaching the aqueous:CCl_4 interface, breaking apart, and allowing all of its monomers to adsorb to the interface. The kinetics of this model can be described by the following expression:

$$\frac{dn(t)}{dt} = -m\frac{dv(t)}{dt} \tag{6}$$

where n(t) and v(t) are the time dependent concentrations of adsorbed monomers and vesicles in the subsurface layer, respectively; m refers to the average number of monomers in a vesicle.

In the low concentration limit the vesicle concentration depends on extent of monolayer formation and follows first order kinetics:

$$\frac{dv(t)}{dt} = kv \tag{7a}$$

$$v(t) = v_o e^{-kt} \tag{7b}$$

Here, k represents the rate constant for vesicle rupture at the interface. Conservation of molecules requires that the number of adsorbed monomers equals the number of ruptured vesicles multiplied by the number of monomers per vesicle (assumed to be a constant):

$$n(t) = m\left(v_o - v(t)\right) = mv_o\left(1 - e^{-kt}\right) \tag{8}$$

According to Eq. 8, the time dependent surface concentration should follow first order kinetics, asymptotically approaching its equilibrium limit according to the rate constant for vesicle decomposition, k. The term mv_o simply reflects the initial bulk PC concentration (which is equal to the initial PC concentration in the subsurface layer).

In the high concentration limit the vesicle concentration remains unchanged and the solution to Eq. 6 for n(t) reduces to pseudo zeroth order kinetics as in Eq. 5.

These two different expressions for n(t) arising from the rupture mechanism demonstrate that the total bulk phosphatidylcholine concentration can play an important role in the rate of monolayer formation. Experimental isotherms for these PC systems above their respective transition temperatures (Fig. 3b, DLPC) show that tightly packed monolayers consist of a total of ~5 x 10^{15} monomers (in 27 cm^2) corresponding to molecular areas of 55 ± 9 $Å^2$/molecule. For 25 ml of a 0.5 μMolar PC solution, ~70% of the molecules in solution would be required to form a tightly packed monolayer. This percentage does not take into account PC monomers which adsorb to the walls of the dish or to the aqueous:air interface. Should these effects prove non-neglible, then higher bulk concentrations would be required in order to form tightly packed monolayers. In fact we do not observe formation of tightly packed monolayers from aqueous solutions of PC vesicles in their liquid crystalline phase until bulk concentrations of ~2μMolar. At this bulk concentration, only ~15% of the PC molecules in solution need to adsorb to the aqueous:CCl_4 interface in order to form a monolayer with the observed surface coverage.

C. Relating n(t) to γ(t): Equations of State

1. Ideal Equation of State

Relating the time dependent surface concentration (Eq. 5 or Eq. 8) to the experimentally measured dynamic surface tension, γ(t), requires choice of an appropriate

two dimensional equation of state. In the simplest case the measured surface tension can be related to the surface concentration by the two dimensional ideal gas equation: [28]

$$\Pi A = n(t)RT \tag{9}$$

where $\Pi = \gamma_o - \gamma(t)$

A = interfacial area (m^2)

$n(t)$ = surface concentration (mole)

$R = 8.314$ $Jmole^{-1}K^{-1}$

T = temperature (K)

The ideal equation of state assumes that the adsorbed molecules are non-interacting and present at low surface concentrations.

2. Frumkin-based Equation of State

As monolayers become more concentrated adsorbed monomers may begin to experience intermolecular interactions leading to a breakdown of Eq. 9. An equation of state based on the Frumkin isotherm takes these forces into account: [28]

$$\Pi A = n^{\infty} RT \ln\left(1 - \frac{n(t)}{n^{\infty}}\right) \tag{10}$$

Here, n^{∞} represents the surface concentration of a tightly packed monolayer.

Substituting the expression for $n(t)$ from either kinetic model (Eq. 5, Eq. 8) into these different equations of state allows one to obtain an analytical means of fitting the dynamic surface tension as a function of time. Table 2 summarizes the results as Equations 11 - 13. Equations are grouped (e.g. Eq. 11a and 11b) according to their analytic functional form. Several sets of conditions predict that the surface tension should depend on time in a linear fashion (Eq. 11a and 11b) : a) the extraction mechanism coupled with

the ideal equation of state; b) the rupture mechanism in the high concentration limit coupled with the ideal equation of state; and c) the rupture mechanism in the low concentration limit coupled with the Frumkin-based equation of state. Assuming the low concentration limit of the rupture mechanism and the ideal equation of state predicts that the surface tension should follow an exponential decay with time (Eq. 12). Lastly, when either the extraction mechanism or the rupture mechanism (high concentration limit) is coupled to the Frumkin based equation of state, $\gamma(t)$ assumes a time dependence which is not easily represented (Eq. 13a). However, this expression can be inverted leading to a simple exponential dependence of time on the measured surface tension. (Eq. 13b and 13c).

IV. Results and Discussion

A. Concentration Dependence of Monolayer Formation

1. Low Concentration Limit

Experiments carried out above the bilayer gel-liquid crystalline transition temperature (T_c) show the rate and extent of monolayer formation to depend quite sensitively on the bulk PC concentration. The DLPC isotherm in Fig. 3b demonstrates how the equilibrium properties of the monolayer change with bulk PC concentration. At bulk concentrations of ≥ 2 μMolar, the terminal surface pressure reaches an asymptotic limit of ~42 mN/m. Further increase in bulk concentration does not lead to any additional increase in surface pressure, indicating an upper limit to the extent of monomer packing at the aqueous:CCl_4 interface. As mentioned in the experimental section, analysis of the DLPC isotherm data by means of the Gibbs equation calculates that these tightly packed monolayers have concentrations of 1.8×10^{14} molecules/cm^2 or, equivalently, molecular areas of 55 Å^2/molecule.[30,31]

Although the equilibrium or terminal surface pressure does not change for bulk PC concentrations above 2 μMolar, the rate at which the monolayers form still depends upon bulk concentration. The upper panel of Figure 5 shows the time dependent surface tension

during monolayer formation from solutions of different bulk DLPC concentrations. At bulk concentrations of ~1 μMolar and below, the data decay in an exponential fashion slowly approaching an asymptotic limit determined by bulk concentration and experimental temperature. The lower panel of Figure 5 shows a expanded view of the 1μMolar system. Indistinguishable from the data at all but the earliest times (≤ 10 min) is the fit to an exponential decay. Except for the earliest times during monolayer formation, the exponential decay reproduces the experimental data to within 0.1 mN/m, well within the limits of experimental uncertainty. This behavior of the surface tension is consistent with Equation 12 which couples the vesicle rupture mechanism to the ideal equation of state.

Fitting the data to a single exponential decay requires that the fit coefficients assume physically meaningful definitions. Equation 12 has the general form:

$$\gamma(t) = a_0 + a_1 e^{-a_2 t} \tag{14}$$

From Eq. 12 we see that a_0 corresponds to (γ_o - RTmv$_o$/A) and a_1 equals RTmv$_o$/A. The term in the exponent, a_2, is simply the rate constant for vesicle rupture, k. In physical terms, a_0 should equal the *equilibrium interfacial tension* for a system with a specified DLPC bulk concentration, a_1 should scale linearly with bulk concentration (according to the mv_0 term) and a_2 is not expected to show any concentration dependence.

Figure 6 plots the fit parameters, a_0, a_1 and a_2, against bulk DLPC concentration. At concentrations below 2 μMolar, the fit parameters behave in the manner predicted by Eq. 12. Fitting the 2 μMolar system leads to a physically unreasonable a_0 value of -5 mN/m while the a_0 parameter for higher concentrations varies without a systematic trend. The a_1 coefficient depends linearly on bulk DLPC concentration up to a bulk concentration of 1.2 μMolar. At concentrations of 2 μMolar and higher the a_1 coefficient levels out at a value of ~30 mN/m. We note that at the lower concentrations, the a_1 coefficients from calculated fits correlate reasonably well with the value one would calculate using the

analytical expression in Eq. 12 ($a_1 = RTmv_0/A$). For example, at a bulk concentration of 1 μMolar, the analytical form of a_1 calculates a value of 20 mN/m while the fit yields a value of 15 mN/m. Given that the model does not take into account loss of PC monomers to the air:aqueous interface or to the walls of the dish, the "effective" PC concentration (mv_0) may very well be lower than the reported concentration. This overestimation of the bulk PC concentration by the analytical expression would lead to a calculated a_1 value which was higher than the value from a fit to Eq. 14 which samples the experimental or effective PC concentration. Finally, the plot of a_2 versus concentration shows the rate constant for monomer adsorption to be constant at sufficiently low concentrations (< 2μMolar). At higher concentrations, the rate constant appears to climb but this observation should be tempered by the fact that at these higher concentrations, Eq. 12 no longer captures the functional form of the dynamic surface tension.

2. High Concentration Limit

At bulk PC concentrations ≥ 2 μMolar the DLPC isotherm (Figure 3b) indicates that the resulting monolayer approaches its tight packed limit. Consequently, the two dimensional ideal equation of state (Eq. 9) should no longer accurately describe the adsorbed monolayer. More appropriate is an equation of state such as Eq. 10 which takes into account intermolecular interactions between monomers at the interface. Because experimental conditions already specify a high concentration of PC vesicles in bulk solution, the expression for the time dependent surface concentration, n(t), does not depend on the choice of mechanism. Both the extraction and the rupture mechanisms express n(t) as a linear function of time (Eq. 5). Substituting into Equation 10 for n(t) leads to an expression of $\gamma(t)$ in terms of time which is not easily represented (Eq. 13a., Table 2). However, Eq. 13a may be inverted to recast time as a function of interfacial tension, γ. Carrying out this operation leads to Eq. 13b/c in Table 2.

Figure 7 shows the results of trying to fit the high concentration surface tension data with Eq. 12 and Eq. 13b/c. By inspection we can eliminate Eq. 11 which predicts linear dependence of $\gamma(t)$ on time. In the top panel of Fig. 7, surface tension is plotted vs. time and the data are fit to a single exponential decay according to Eq 12. Although the differences between calculated and experimental surface tensions never grow larger than 1.5 mN/m, close analysis reveals that the fit deviates from the data in a systematic fashion and never accurately describes the time dependent behavior of the surface tension. In the bottom panel the experimental time is plotted versus the measured surface tension and the data is fit according to Eq. 13b/c. Between surface tensions of 43 mN/m (t = 0) and 6 mN/m (t = 120 min) the fit is virtually indistinguishable from the data. We take the remarkable correlation between the experimental data and the calculated fit as an indication that Equation 13b/c does, in fact, accurately capture the important aspects of the monolayer formation process in the high aqueous PC concentration limit. Furthermore, if one assumes the vesicle rupture mechanism, then the rate constant, k ($=n^{\infty}/a_0 m v_0$) agrees with vesicle rupture rate constants taken from the exponential term in the low concentration experiments. This high concentration rate constant appears as the open triangle in Fig. 5c.

After the first two hours of the 8 μMolar experiment, the surface tension slowly decays from 6 mN/m to 4 mN/m in a manner inconsistent with the analysis between 0 min $\leq t \leq$ 120 min. This behavior suggests a crossover in the mechanism of monolayer formation, possibly from the proposed rupture mechanism to more of an extraction type mechanism. Intuitively, such a crossover seems reasonable given that during the latter stages of monolayer formation at high PC concentrations, vesicles no longer approach a neat aqueous:CCl_4 interface. Rather, vesicles see a moderately packed sheet of PC headgroups, and the limiting constraint on the monolayer formation kinetics may simply become creating space to accommodate the remaining monomers.

Although Figure 7 supports using the Frumkin based equation of state (Eq. 10) for describing monolayer formation kinetics in the high concentration limit, the analysis can not

distinguish which mechanism leads to monolayer formation. At high concentrations the extraction and the rupture mechanisms predict a linear time dependence for n(t) (Eq. 5) and, consequently, similar expressions for $\gamma(t)$ (Eq. 11, Eq. 13b and 13c). The only difference between Eq. 13b and Eq. 13c lies in a factor of m, the number of monomers per vesicle which we assume to be an ensemble averaged constant. However, we believe that the rupture mechanism represents the primary source by which monolayers form in the high concentration limit based on data from the low concentration experiments. At low concentrations only the rupture mechanism coupled with the ideal equation of state leads to an analytic expression (Eq. 12) which accurately fits the experimental dynamic surface tension data. *A priori* we see no reason to assume that the mechanism during the initial stages of monolayer formation should change with increasing PC concentration. Agreement of the one adjustable parameter in Eqs. 12 and 13c, the rate constant for vesicle rupture k, strengthens this claim. We therefore propose that monolayer formation initially proceeds by means of vesicle rupture. Only in the latter stages of monolayer formation from solutions having high PC concentrations do we expect the rupture mechanism to give way to an extraction type of mechanism.

B. Dependence of Monolayer Formation on PC bilayer Phase

The previous section provided evidence supporting the rupture mechanism as the means by which PC monolayers form at an aqueous:CCl_4 interface from a solution of aqueous phase, liquid crystalline vesicles. Dynamic surface tension experiments in both the low and high concentration limits were consistent with predictions of the rupture mechanism coupled with the appropriate equations of state. We now show how both the rate and extent of monolayer formation depends sensitively on lipid bilayer phase. Figure 8 contains time dependent surface tension data for 1μMolar solutions of DLPC (n = 12), DMPC (n = 14), DPPC (n = 16) and DSPC (n = 18) at 22° C. Shown are the first 10 hrs of each experiment as well as the asymptotic surface tension limits for each system. The

time required to reach these limits varies from ~24 hrs (DLPC) to ≥ 72 hrs (DSPC and DPPC systems). Three days marked the limit of our ability to collect reliable data from a single experiment. After three days the age of the interface became a concern and evaporative losses began to play a role in the surface tension measurements.

The data in Fig. 8 clearly show that at room temperature the extent of monolayer formation depends inversely on the hydrocarbon chain length of the PC species. DLPC forms the most concentrated monolayer, while DPPC and DSPC form the most expanded monolayers. Transition temperatures in Table 1 show that for these ambient experiments (T = 22° C), the DLPC solution contains vesicles in their more fluid, liquid crystalline phase. DMPC vesicles exist in a liquid crystalline/gel coexistence region while DPPC and DSPC vesicles are frozen with their lipid bilayers in a rigid gel phase. Despite these differences the systems do share similarities. Most notably, surface tension experiments show evidence that monolayer formation remains barrier controlled regardless of vesicle bilayer phase, and kinetics in the low concentration limit always appear to be first order in bulk PC concentration.

Both the DSPC isotherm (Fig 3b.) and the time dependent surface tension data suggest that PC vesicle solutions below T_c can only form expanded monolayers and the monolayers themselves form very slowly. In earlier work we demonstrated how the extent of monolayer formation changes discontinuously at the gel/liquid crystalline transition temperature.[31] At temperatures above their respective transition temperatures, PC solutions with concentrations ≥ 2 μMolar irreversibly form monolayers with surface coverages of 55 Å^2/molecule. Below T_c PC solutions form expanded monolayers regardless of bulk concentration provided that the monolayers are allowed to form without external perturbation. Recent work in this lab has shown that physically disturbing the interface following partial monolayer formation can produce compact monolayers even at temperatures below T_c.[52] Under such circumstances monolayers of longer chain species exhibit characteristics consistent with very tightly packed monomers.

C. Temperature Dependence of Monolayer Formation

The dynamic surface tension experiments suggest fundamental differences in the monolayer formation process depending on whether the experimental temperature lies above or below T_c. Although low concentration data support the rupture mechanism (Eq. 12) regardless of bilayer phase, rupture of a liquid crystalline vesicle may proceed in a very different manner than rupture of a gel phase vesicle. In order to examine the effects of the lipid bilayer phase on monolayer formation, we measured the dynamic surface tension of the four PCs in the low concentration limit at different temperatures.

Figure 9 shows representative dynamic surface tension data for 0.5 μMolar DLPC solutions as a function of temperature. Included on the graph are the exponential decays which result from fitting the data to Eq. 12. All four experiments exhibit exponential decay behavior, and from the fit parameters emerges the temperature dependence of the monolayer formation rate. Plotting the natural log of the rate constant (a_2) against inverse temperature generates an Arrhenius plot from which an activation energy for monolayer formation may be calculated.

Arrhenius plots for all four phosphatidylcholines appear in Figure 10 and the results are summarized in Table 3. The liquid crystalline DLPC data (Fig. 10a) lead to a monolayer formation activation energy (E_a) of 39 ± 7 kJ/mol. Activation energies for both gel phase DPPC (Fig. 10c) and gel phase DSPC (Fig. 10d) are considerably lower, 17 ± 6 kJ/mol and 20 ± 11 kJ/mol, respectively. The C_{14} species, DMPC, affords a unique opportunity to explicitly examine how the phase of the lipid bilayer affects the monolayer formation process. With a T_c of 23° C the temperature dependence of monolayer formation kinetics can be examined for solutions of vesicles both in the rigid gel phase (T < 23° C) and in the more fluid, liquid crystalline phase (T > 23° C). The DMPC kinetic data (Fig. 10b) show a break in the Arrhenius plot at approximately the DMPC transition temperature. Monolayer formation from aqueous solutions of liquid crystalline vesicles has an E_a of 41 ±

8 kJ/mol, effectively identical to that of DLPC. However, for solutions of vesicles in their gel state, E_a drops by a factor of five to 8 ± 5 kJ/mol. Generally speaking, E_a appears to be larger for solutions of liquid crystalline vesicles than for solutions of gel phase vesicles.

While studying rates of phosphatidylcholine monomer exchange between unilamellar vesicles, McLean and Phillips observed similar, lipid bilayer phase dependent behavior.[22] Specifically, exchange kinetics of DMPC monomers between DMPC vesicles in their liquid crystalline phase exhibited a much stronger temperature dependence than did monomer exchange between gel phase vesicles. The calculated activation energies for monomer exchange were 70 kJ/mol for exchange between liquid crystalline vesicles and 47 kJ/mol for gel phase vesicles.[22] Although both of these values lie considerably higher than the calculated activation energies for monolayer formation (41 kJ/mol liquid crystalline, 8 kJ/mol gel) the trend of a larger barrier for liquid crystalline systems is consistent with the results of the temperature dependent dynamic surface tension experiments. Quantitative differences in the energetics of the two processes - monomer exchange and monolayer formation - may arise due to the different mechanisms by which the two phenomena proceed. Monomer exchange between vesicles necessarily requires an extraction/insertion type mechanism[20] while the dynamic surface tension experiments discussed in the previous sections suggest that monolayer formation proceeds via vesicle rupture. If monomer insertion into a host bilayer has a large energetic barrier relative to adsorption at the aqueous:CCl_4 interface, then one would expect monomer exchange to have higher activation energies than monolayer formation.

Despite differences between the mechanisms of monomer exchange and monolayer formation, we expect the concepts used to explain the phase dependent activation energies to transfer between the two phenomena. Based on earlier work carried out on micellar dynamics,[53] McLean and Phillips postulated that the smaller barrier for exchange between gel phase vesicles arose from the high degree of order amongst the acyl chains within the bilayer.[22] A phospholipid monomer contained within a gel phase bilayer already has its

chains aligned in all-*trans* conformations and can easily slide out of the bilayer into solution given a strong enough chemical driving force. [4,5,54] In contrast acyl chains of a phospholipid monomer in a liquid crystalline bilayer are considerably more disordered and require straightening before the monomer can separate from the vesicle wall.[54,55] (See, for example, Fig. 2b.) This additional energy needed to straighten the chains of the departing monomer leads to the higher activation energy for monomer exchange between liquid crystalline vesicles.[53]

By analogy, we speculate that gel phase vesicles face a smaller barrier to vesicle rupture at the aqueous:CCl_4 interface due to the well ordered, all-*trans* hydrocarbon chains which make up the bilayer interior. The rigid, gel phase vesicles will be more susceptible to vesicle fracture than the more fluid liquid crystalline vesicles whose bilayer interiors possess a much higher degree of disorder. In liquid crystalline vesicles acyl chain entanglement and flexibility should inhibit vesicle rupture at the interface which results in a higher activation energy for monolayer formation. We note that if the nature of vesicle rupture changes as vesicles pass from the gel state to the liquid crystalline state, we might expect to see this effect appear in the rate of monolayer formation at T_c. The DMPC data in Figure 9b provide evidence of such a change with the rate constant for monolayer formation just below T_c being slightly - but reproducibly - larger than the rate constant just above T_c. At T_c monolayer formation from gel phase vesicles should proceed more quickly than from liquid crystalline vesicles due to the differences in the monolayer formation activation energies.

The disparity E_a for gel vs. liquid crystalline phase vesicles prompts the question of why gel phase vesicles with a smaller barrier to monolayer formation only form expanded monolayers regardless of bulk PC concentration, while liquid crystalline vesicles form tightly packed monolayers at bulk PC concentrations above 2 μMolar. Resolving this paradigm requires treating monolayer formation as a thermodynamically driven process where energetics of initial states (monomers in vesicles) and final states (monomers in

monolayers) must be considered. Figure 11 depicts a schematic diagram illustrating the monolayer formation process. The vesicle rupture reaction coordinate appears on the abscissa while the ordinate represents the internal energy of the reactants and the products. When a system of vesicles lies just above and just below T_c, liquid crystalline vesicles are energetically separated from gel phase vesicles by ΔH_{fus} for the gel-liquid crystalline phase transition, a quantity measured in differential scanning calorimetry (DSC) experiments.[56,57] DSC data for the four phosphatidylcholines studied show ΔH_{fus} to be 17 kJ/mol for DLPC, 26 kJ/mol for DMPC, 40 kJ/mol for DPPC, and 45 kJ/mol for DSPC.[56,57]

Appearing between the initial and final states of the vesicle/interface system are the barriers to gel and liquid crystalline vesicle rupture. The Arrhenius data in Figure 10 and Table 3 show the barrier to be 2-5 times larger for solutions of liquid crystalline vesicles than for solutions of vesicles in their gel phase. In order for a monolayer to form, this barrier must be overcome. This picture may oversimplify the actual monolayer formation process in the limit when tightly packed monolayers form from solutions of liquid crystalline vesicles. Such circumstances may require that a second barrier appear in order to represent adsorption of monomers after the monolayer has mostly formed. The high concentration data in Figure 7b already hint that the mechanism changes during the latter stages of monolayer formation (at $t > 120$ min). However, in the low concentration limit, we assume that if a vesicle ruptures at the interface, its monomers adsorb without having to overcome any further kinetic or thermodynamic barriers.

On the right hand side of Figure 11 are different stages of PC monolayer formation. As the monolayer becomes more concentrated (as more monomers adsorb to the interface) the internal energy of the monolayer rises. We stress that this picture does not attempt to quantitatively relate the internal energies of the gel and liquid crystalline vesicles to the internal energies of the different monolayer states. Nevertheless, we may draw several qualitative conclusions from Figure 11: when faced with a neat aqueous:CCl_4 interface,

solutions of PC vesicles experience a driving force to rupture and form monolayers regardless of lipid bilayer phase. Initially, vesicle rupture probably represents an entropically driven process. The system will become increasingly disordered as the first vesicles disintegrate depositing their monomers at the interface. Enthalpic contributions to vesicle rupture and monomer adsorption probably cancel out given that heats of solvation for alkyl chains in hydrocarbon liquids and CCl_4 are similar.[58]

As the monolayer forms, its internal energy rises just as in Langmuir trough compression experiments. (In Langmuir trough experiments,[36] the number of adsorbed monomers remains constant while the monolayer area changes; in these dynamic surface tension experiments, the area remains unchanged while the number of adsorbed monomers increases.) Eventually, the internal energy of the adsorbed monolayer equals that of the gel phase vesicle and the driving force responsible for gel phase vesicle rupture abates. Vesicles in their liquid crystalline phase, however, lie higher in energy thus they will continue to rupture forming an increasingly concentrated monolayer.

V. Conclusions

This paper has presented dynamic surface tension experiments which examine the formation of phosphatidylcholine monolayers at an aqueous:carbon tetrachloride interface from solutions of PC vesicles by means of the Wilhelmy plate method. Results show that monolayer formation represents an activated rather than a diffusion controlled process. A number of different variables control the rate of formation including aqueous phosphatidylcholine concentration, temperature and vesicle bilayer phase.

The rate at which these monolayers form can be quantitatively described by means of a simple first order kinetic model which assumes that vesicles rupture at a planar boundary between the two immiscible liquids. By this model every rupture event allows a vesicle's monomers to adsorb to the interface. In order to relate the time dependent surface concentration, n(t), to the experimentally measured time dependent surface tension ($\gamma(t)$),

the two quantities must be related by an appropriate two dimensional equation of state. We demonstrated that the two dimensional ideal gas law describes the expanded monolayer experimental data with remarkable accuracy. As the monolayer grows more concentrated, the ideal gas law begins to break down requiring the use of a Frumkin based equation of state. These results appeal to intuition: at low surface concentrations we would expect the adsorbed monomers to be non-interacting, while at higher surface concentrations intermolecular interactions between the adsorbed monomers should begin to affect monolayer characteristics.

Both dynamic surface tension measurements (Fig. 7) and equilibrium isotherms (Fig. 3b) show that the vesicle bilayer phase plays an important role in determining the rate and extent of monolayer formation. For experiments carried out above the vesicle bilayer gel-liquid crystalline transition temperature, T_c, tightly packed monolayers form at bulk concentrations greater than 2 μMolar and the equilibration time is comparatively short . Experiments carried out at temperatures below T_c lead to expanded monolayers regardless of bulk PC concentration and experiments require days to approach an asymptotic limit. Nevertheless, monolayer formation remains barrier controlled regardless of vesicle bilayer phase and the rate of monolayer formation still behaves in a manner consistent with the rupture mechanism. These observations suggest that vesicle rupture happens differently for gel and liquid crystalline vesicles.

In order to examine further the effects of vesicle bilayer phase on phosphatidylcholine monolayer formation, we carried out dynamic surface tension experiments at different temperatures for all four PCs. Monolayer formation from solutions of liquid crystalline vesicles had a relatively large activation energy of ~40 kJ/mol while monolayer formation from gel state vesicles was considerably lower (8-20 kJ/mol). Solutions of DMPC vesicles provided the most striking example of this trend: below T_c formation of a DMPC monolayer encounters an energetic barrier of 8 kJ/mol while above T_c the activation energy climbs by a factor of five to 41 kJ/mol. Other studies examining

intervesicle monomer exchange have encountered a similar phenomenon, namely monomer exchange between gel phase vesicles had a much smaller E_a than monomer exchange between liquid crystalline vesicles. Both the monolayer formation and the monomer exchange results can be understood in terms of the ordering amongst hydrocarbon chains comprising the vesicle bilayer. Gel phase vesicles have well ordered, rigid bilayer interiors which may be more brittle and prone to rupture in the energetically anisotropic environments presented by interfaces. Bilayers in liquid crystalline vesicles are more disordered and flexible, resulting in a larger barrier to vesicle rupture. The propensity of liquid crystalline vesicles to form tightly packed monolayers may reflect the energetics of the initial and final states (vesicles and monolayers) in the monolayer formation process.

This study marks the first attempt to quantitatively describe the formation of phosphatidylcholine monolayers at a planar liquid:liquid interface from solutions of PC vesicles. While the models in this paper provide a consistent, satisfactory explanation of the data, several extensions of this work immediately suggest themselves. To test the generality of the methods described above, similar analyses can be performed incorporating different two dimensional equations of state or new mechanisms of monolayer formation. Experimental extensions involve tailoring the composition of the vesicle bilayers to affect the rate of monolayer formation as well as investigating the structural integrity of vesicles after incorporating biological macromolecules into the bilayer.

Acknowledgments

The authors thank Dr. Beth Smiley for helpful discussions and Julie Gruetzmacher for carrying out some of the early temperature dependent surface tension measurements. Funding from the National Science Foundation (CHE-9725751) and the Office of Naval Research is gratefully acknowledged.

Bibliography

1) Jones, M. N.; Chapman, D. *Micelles, Monolayers and Biomembranes*; John Wiley & Sons: New York, 1995.

2) Safran, S. A. *Statistical thermodynamics of surfaces, interfaces, and membranes*; Addison-Wesley: New York, 1994; Vol. 90.

3) Arora, A.; Gupta, C. M. *Biochim. Biophys. Acta* **1997**, *1324*, 47-60.

4) Gericke, A.; Moore, D. J.; Erukulla, R. K.; Bittman, R.; Mendelsohn, R. *J. Mol. Struc.* **1996**, *379*, 227-239.

5) Mendelsohn, R.; Davies, M. A.; Brauner, J. W.; Schuster, H. F.; Dluhy, R. A. *Biochemistry* **1989**, *28*, 8934-8939.

6) Huang, C.; Mason, J. T.; Levin, I. W. *Biochemistry* **1983**, *22*, 2775-2780.

7)Frokjaer, S.; Hjorth, E. L.; Worts, O. *Stability Testing of Liposomes during Storage*; Frokjaer, S.; Hjorth, E. L.; Worts, O., Ed.; CRC Press: Boca Raton, FL, 1984; Vol. 1, pp 235-244.

8) Litzinger, D. C.; Huang, L. *Biochim. Biophys. Acta* **1992**, *1113*, 201-227.

9) Gregoriadis, G. *Targeted drug delivery and biological interaction*; CRC Press: Boca Raton, 1984; Vol. 3.

10) Lasic, D. D.; Papahadjopoulos, D. *Science* **1995**, *267*, 1275-1276.

11) Szoka, F.; Papahadjopoulos, D. *Ann. Rev. Biophys. Bioeng.* **1980**, *9*, 467-508.

12) Gregoriadis, G. *Preparation of Liposomes*; CRC Press: Boca Raton, 1984; Vol. 1.

13) Pattus, F.; Desnuelle, P.; Verger, R. *Biochim. Biophys. Acta* **1978**, *507*, 62-70.

14) Schindler, H. *Biochim. Biophys. Acta* **1979**, *555*, 316-336.

15) Williams, L. M.; Evans, S. D.; Flynn, T. M.; Marsh, A.; Knowles, P. F.; Bushby, R. J.; Boden, N. *Langmuir* **1997**, *13*, 751-757.

16) Nag, K.; Perez-Gil, J.; Cruz, A.; Rich, N. H.; Keough, K. M. W. *Biophys. J.* **1996**, *71*, 1356-1363.

17) Ivanova, T.; Raneva, V.; Panaiotov, I.; Verger, R. *Colloid and Polymer Science* **1993**, *271*, 290-297.

18) Yang, E.; Huestis, W. H. *Biochemistry* **1993**, *32*, 12218-12228.

19) Vaz, W. L. C.; Clegg, R. M.; Hallman, D. *Biochemistry* **1985**, *24*, 781-786.

20) Pownall, H. J.; Bick, D. L. M.; Massey, J. B. *Biochemistry* **1991**, *30*, 5696-5700.

21) Nichols, J. W. *Biochemistry* **1985**, *24*, 6390-6398.

22) McLean, L. R.; Phillips, M. C. *Biochemistry* **1984**, *23*, 4624-4630.

23) Doody, M. C.; Pownall, H. J.; Kao, Y. J.; Smith, L. C. *Biochemistry* **1980**, *19*, 108-116.

24) Bayerl, T. M.; Schmidt, C. F.; Sackmann, E. *Biochemistry* **1988**, *27*, 6078-6085.
25) Laughlin, R. G. *Colloid Surf. A.* **1997**, *128*, 27-38.
26) MacDonald, R. C.; Simon, S. A. *Proc. Nat. Acad. Sci., USA* **1987**, *84*, 4089-4093.
27) Brown, R. E. *Biochim. Biophys. Acta* **1992**, *1113*, 375-389.
28) Adamson, A. W. *Physical Chemistry of Surfaces*; 4 ed.; John Wiley & Sones: New York, 1982.
29) Qui, R.; MacDonald, R. C. *Biochim. Biophys. Acta* **1994**, *1191*, 343-353.
30) Walker, R. A.; Gruetzmacher, J. A.; Richmond, G. L. *Journal of the American Chemical Society* **in press**.
31) Walker, R. A.; Conboy, J. C.; Richmond, G. L. *Langmuir* **1997**, *13*, 3070-3073.
32) Walker, R. A.; Gragson, D. E.; Richmond, G. L. **submitted**.
33) Grandell, D.; Murtomaki, L. *Langmuir* **1998**, *14*, 556-559.
34) Li, J.; Fainerman, V. B.; Miller, R. *Langmuir* **1996**, *12*, 5138-5142.
35) Stigter, D.; Mingins, J.; Dill, K. A. *Biophys. J.* **1992**, *61*, 1603-1615.
36) Mingins, J.; Taylor, J. A. G.; Pethica, B. A.; Jackson, C. M.; Yue, B. Y. T. *J. Chem. Soc. Faraday Trans. I* **1982**, *78*, 323-339.
37) Throughout this paper the term "tightly packed" refers to monolayers having concentrations of 1.8×10^{14} molecules/cm^2 or, equivalently, 55 Å^2/molecule. Without external means for monolayer compression, we rely on the equilibrium existing between aqueous phase PC vesicles and adsorbed PC monomers to create monolayers having different surface concentrations. The most tightly packed monolayer formed under these circumstances has a molecular area of 55 Å^2/molecule regardless of chain length.
38) Eastoe, J.; Dalton, J. S.; Rogueda, P. G. A.; Griffiths, P. C. *Langmuir* **1998**, *14*, 979-981.
39) Brinck, J.; Jönsson, B. *Langmuir* **1998**, *14*, 1058-1071.
40) Diamant, H.; Andelman, D. *J. Phys. Chem.* **1996**, *100*, 13732-13742.
41) Ravera, F.; Liggieri, L.; Steinchen, A. *J. Colloid Interface Sci.* **1993**, *156*, 109-116.
42) Bychuk, O. V.; O'Shaughnessy, B. *J. Colloid Interface Sci.* **1994**, *167*, 193-203.
43) Motomura, K. *J. Colloid Interface Sci.* **1978**, *64*, 348-361.
44) Rillaerts, E.; Joos, P. *J. Phys. Chem.* **1982**, *86*, 3471-3478.
45) Ward, A. F. H.; Tordai, L. *J. Chem. Phys.* **1946**, *14*, 453-461.
46) Makievski, A. V.; Fainerman, V. B.; Miller, R.; Bree, M.; Liggieri, L.; Ravera, R. *Colloid Surf. A.* **1997**, *122*, 269-273.
47) VanHunsel, J.; Bleys, G.; Joos, P. *J. Colloid Interface Sci.* **1986**, *114*, 432-441.
48) Joos, P.; Vollhardt, D.; Vermeulen, M. *Langmuir* **1990**, *6*, 524-525.

49) Joos, P.; Uffelen, M. V.; Serrien, G. *J. Colloid Interface Sci.* **1992**, *152*, 521-533.
50) Kakiuchi, T.; Yamane, M.; Osakai, T.; Senda, M. *Bull. Chem. Soc. Jpn.* **1987**, *60*, 4223-4228.
51) Fainerman, V. D.; Makievski, A. V.; Miller, R. *Colloid Surf. A.* **1994**, *87*, 61.
52) Smiley, B. L.; Richmond, G. L. *submitted* .
53) Aniansson, E. A. G.; Wall, S. N.; Almgren, M.; Hoffman, H.; Kielmann, I.; Ulbricht, W.; Zana, R.; Lang, J.; Tondre, C. *J. Phys. Chem.* **1976**, *80*, 905-922.
54) Tieleman, D. P.; Berendsen, H. J. C. *J. Chem. Phys.* **1996**, *105*, 4871-4880.
55) Nagle, J. F.; Zhang, R.; Nagle, S. T.; Sun, W.; Petrache, H. I.; Suter, R. M. *Biophys. J.* **1996**, *70*, 1419-1431.
56) Finegold, L.; Singer, M. A. *Biochim. Biophys. Acta* **1986**, *855*, 417-420.
57) Hinz, H. J.; Sturtevant, J. M. *J. Biol. Chem.* **1972**, *247*, 6071-6075.
58) Fuchs, R.; Chambers, E. J.; Stephenson, W. K. *Can. J. Chem.* **1987**, *65*, 2624-2627.

Table 1. Properties of Phosphatidylcholines

Molecule	n	T_c[56]
DLPC	12	-1° C
DMPC	14	23° C
DPPC	16	41° C
DSPC	18	54° C

Table 2. Expressions for $\gamma(t)$ from extraction and rupture mechanisms coupled with ideal and Frumkin equations of state.

Equation of State	Mechanism: Extraction	Mechanism: Rupture
Ideal	$\gamma(t) = \gamma_o - \frac{RTkv_o}{A}t$ (Equation 11a)	low concentration: $\gamma(t) = \gamma_o - \frac{RTmv_0}{A}\left(1 - e^{-kt}\right)$ (Equation 12)
		high concentration: $\gamma(t) = \gamma_o - \frac{RTkmv_o}{A}t$ (Equation 11b)
Frumkin	$\gamma(t) = \gamma_o + \frac{RTn^\infty}{A}\ln\left(1 - \frac{kv_o t}{n^\infty}\right)$ (Equation 13a)	low concentration: $\gamma(t) = \gamma_o - \frac{RTkmv_o}{A}t$ (Equation 11b)
	$t = \frac{n^\infty}{kv_o}\left(1 - e^{\frac{-\gamma_o}{RTn^\infty}} e^{\frac{\gamma(t)}{RTn^\infty}}\right)$ (Equation 13b)	high concentration: $t = \frac{n^\infty}{kmv_o}\left(1 - e^{\frac{-\gamma_o}{RTn^\infty}} e^{\frac{\gamma(t)}{RTn^\infty}}\right)$ (Equation 13c)

Table 3: Activation energies for monolayer formation

Molecule	Bilayer phase	E_a (kJ/mol)
DLPC	liquid crystalline	39 ± 7
DMPC	liquid crystalline	41 ± 8
	gel	8 ± 5
DPPC	gel	17 ± 6
DSPC	gel	20 ± 11

Figure Captions

Figure 1. Illustration of PC monolayer formation at an aqueous:carbon tetrachloride interface from a solution of PC vesicles. Based on dynamic light scattering measurements, we believe the vesicles used in these studies are multilamellar rather than unilamellar in nature.

Figure 2. a) Phosphatidylcholine structure b) Schematic picture illustrating the gel-liquid crystalline transition in vesicle bilayers. Table 1 contains the transition temperatures, T_c, for the phosphatidylcholines studied in this work.

Figure 3. a) Schematic representation of the Wilhelmy plate method for measuring the tension of the aqueous: carbon tetrachloride interface. In this picture, the aqueous phase wets the platinum plate exerting an upward force which equals the product of the tension and the plate perimter. b) Isotherms for DLPC and DSPC under ambient conditions (22° C). Solutions of DLPC vesicles form tightly packed monolayers (1.8×10^{14} molecules/cm^2 or 55 Å^2/molecule) at concentrations above ~2 μMolar. Solutions of DSPC vesicles form expanded monolayers (as evidenced by lower surface pressures) regardless of bulk concentration.

Figure 4. a) Dynamic surface tension versus time $(\text{min})^{-1/2}$. If monolayer formation followed diffusion controlled kinetics in the long time limit, the data would be linear, especially near the origin. The data begins at t = 90 min (far right) as marked in Fig. 4c. b) Dynamic surface tension versus time $(\text{min})^{1/2}$. Curvature in the data indicate that monolayer formation does not follow diffusion controlled kinetics in the short time limit. c) Dynamic surface tension (solid line) versus time (min) and the fit of the data to a single exponential decay (dashed line). The arrow marks the starting point of the data shown in Fig. 4a. Note that the data extends out to ten hours.

Figure 5. a) Dynamic surface tension data from DLPC solutions with varying bulk DLPC concentrations. b) The first six hours of a DLPC dynamic surface tension experiement in the low concentration limit (same data as in Figure 4). Data were fit to a single exponential decay (dotted line) as predicted by Equation 12 in Table 2.

Figure 6. Fit parameters a_0, a_1, and a_2 from fitting DLPC dynamic surface tension data with Equation 12. Fit parameters agree with analytically calculated values through bulk DLPC concentrations of ~1 μMolar. Also plotted on the a_2 graph as an open triangle is the rate constant, k, calculated from fitting the 8 μMolar data to Equation 13b. Agreement between the high concentration rate constant and rate constants calculated via Equation 13b and the low concentration rate constants calculated via Equation 12 support the idea that monolayer formation proceeds via the rupture mechanism.

Figure 7. a) Dynamic surface tension data for 8 μMolar DLPC plotted versus time according to Equation 12. Although the exponential decay (dashed line) captures the general behavior of the data, it systematically misses the data at the points of steepest descent. b) Experimental time vs. surface tension data for 8 mMolar DLPC with exponential fit as predicted by Equation 13b. The exponential behavior of t(g) through t = 120 minutes (dashed line) exhibits remarkably good agreement with experimental data. After 2 hrs the rate of surface tension decay slows dramatically and approaches the asymptotic limit characteristic of tightly packed monolayers. See text for details.

Figure 8. Dynamic surface tension data for DLPC, DMPC, DPPC, and DSPC under ambient conditions (22° C) and at a bulk concentration of 1 μMolar. Also appearing are the assymptotic equilibrium surface tensions of these systems.

Figure 9. Dynamic surface tension data of DLPC in the low concentration limit at several different temperatures. Also plotted are the exponential decays predicted by Equation 12 Discontinuities in the 38° C data result from the gradual growth and sudden release of carbon tetrachloride vapor bubbles. From the exponential fits come rate constants for monolayer formation according to Eq. 14.

Figure 10. Arrhenius plots of the monolayer formation rate constants for the four phosphatidylcholines examined in this work. Activation energies are calculated from straight line fits to the data. Note the discontinuity in the DMPC data where the slope changes at T_c for the DMPC gel-liquid crystalline bilayer melting transition. See text for details.

Figure 11. Proposed energetics of the monolayer formation process at an aqueous:CCl_4 interface from a solution of PC vesicles. The ordinate plots the internal energies of gel and liquid crystalline phase vesicles as well as the internal energies of the different stages of monolayer formation. Internal energies of the vesicles and monolayers are not quantitatively related on this scale. Along the abscissa lies the vesicle rupture/monolayer formation coordinate.

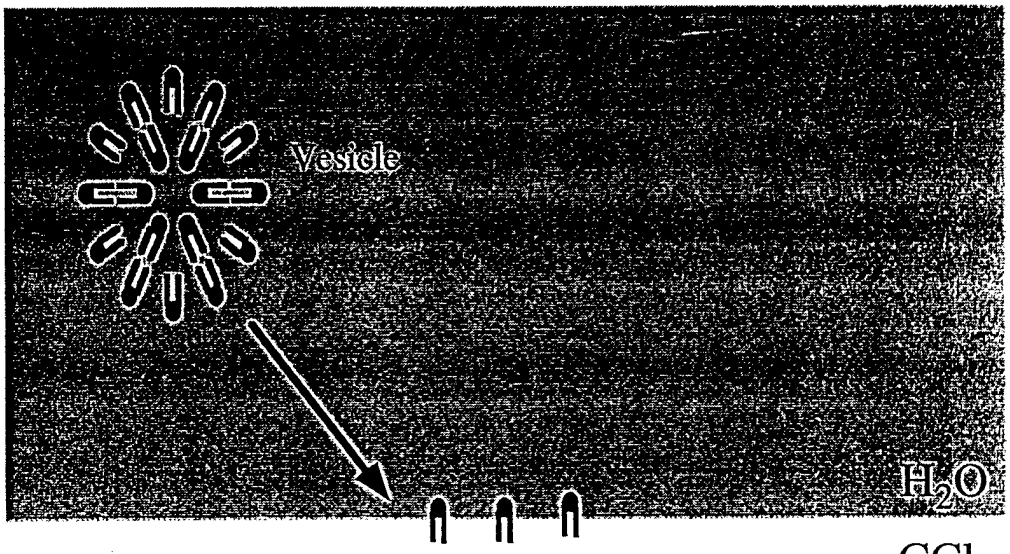

Walker and Richmond

Figure 1

(a)

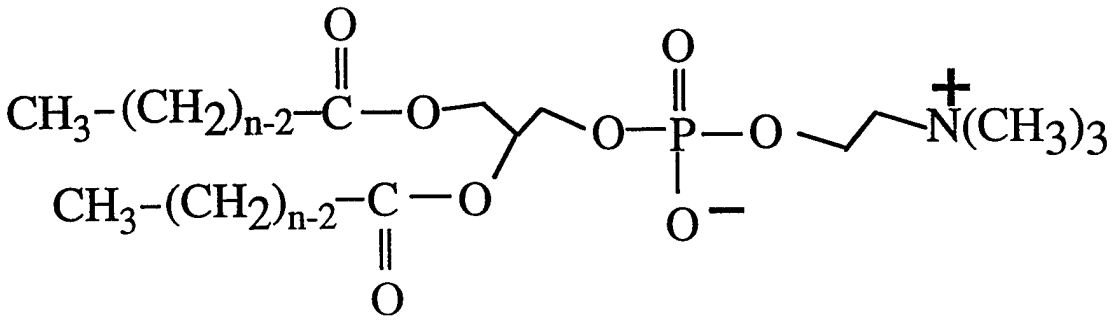

(b)

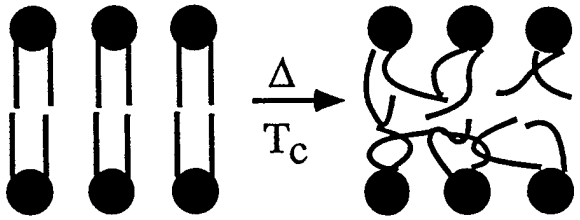

Walker and Richmond

Figure 2

(a)

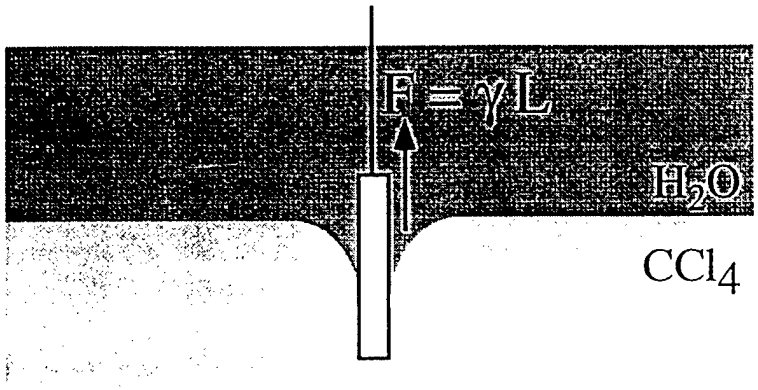

(b)

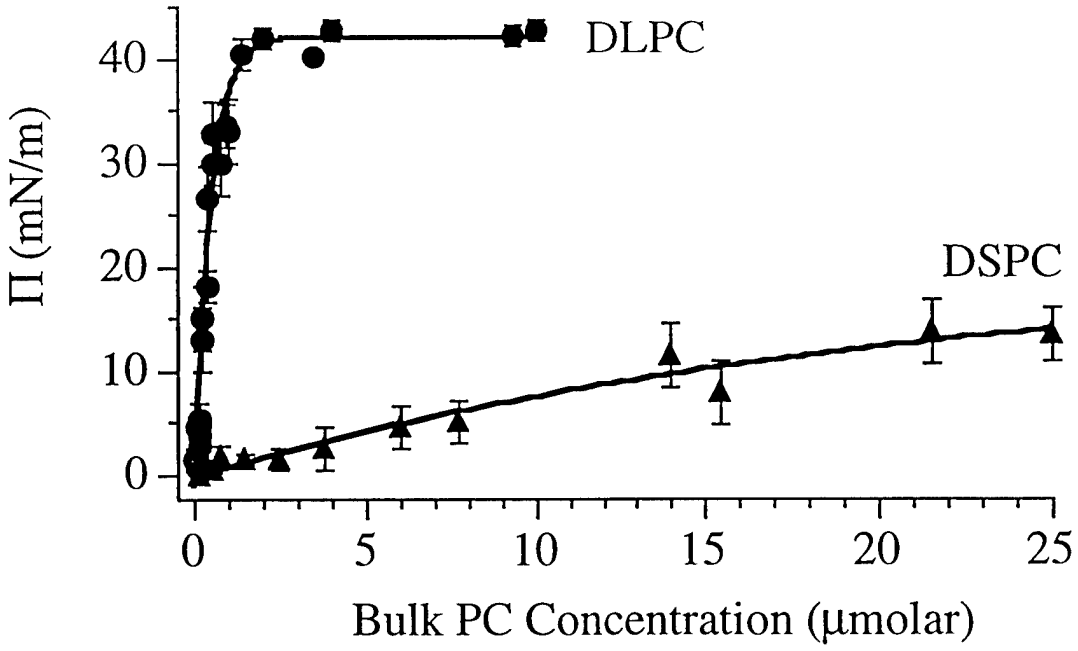

Walker and Richmond

Figure 3

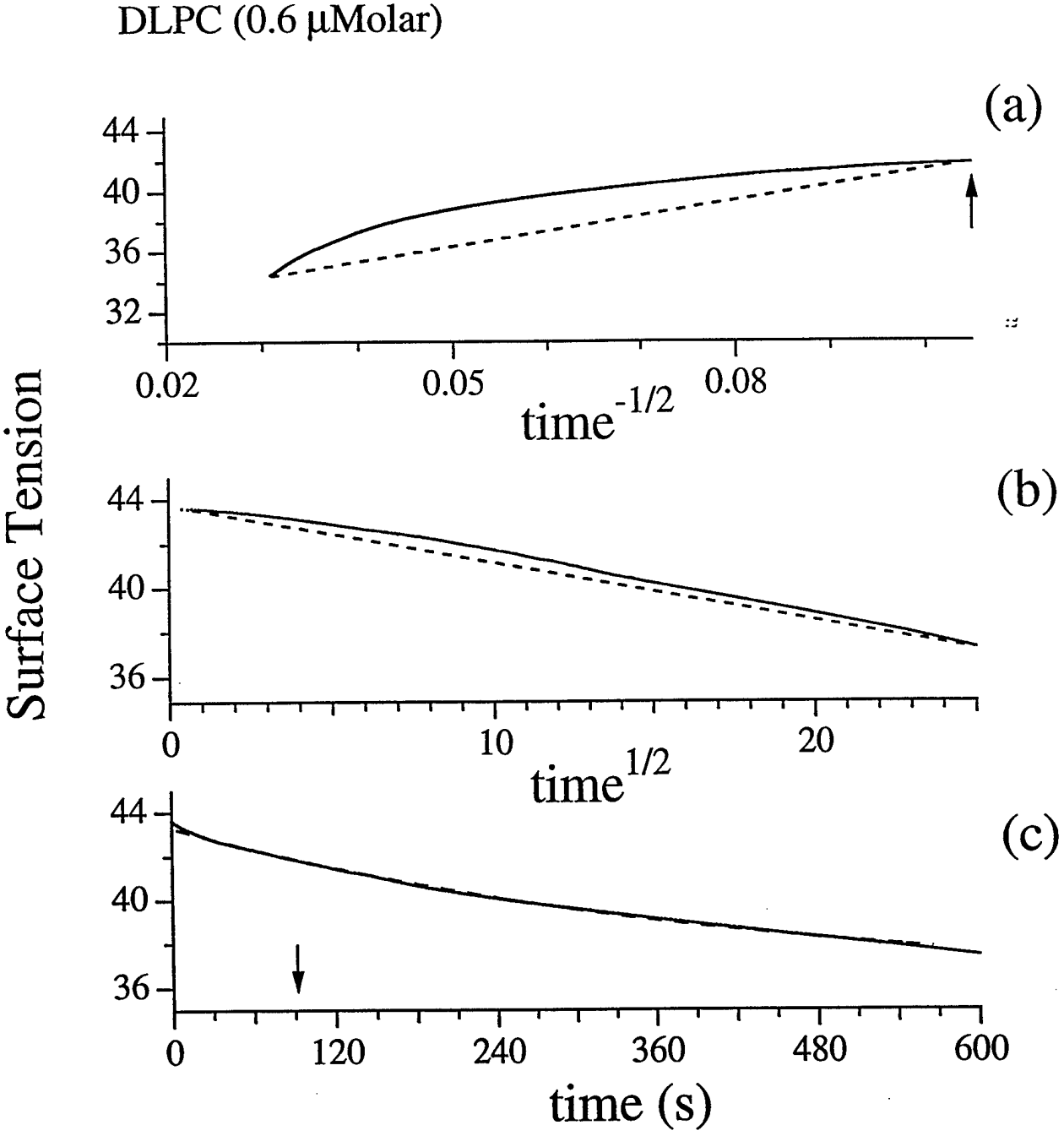

Walker and Richmond
Figure 4

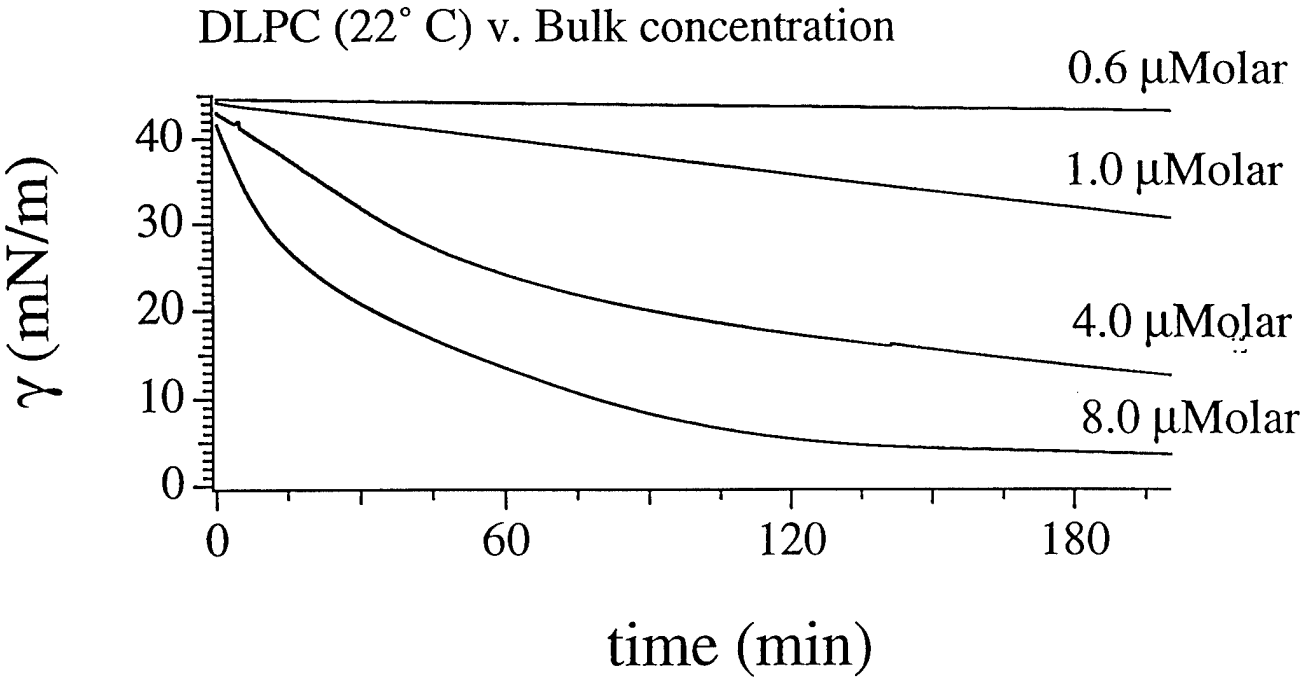

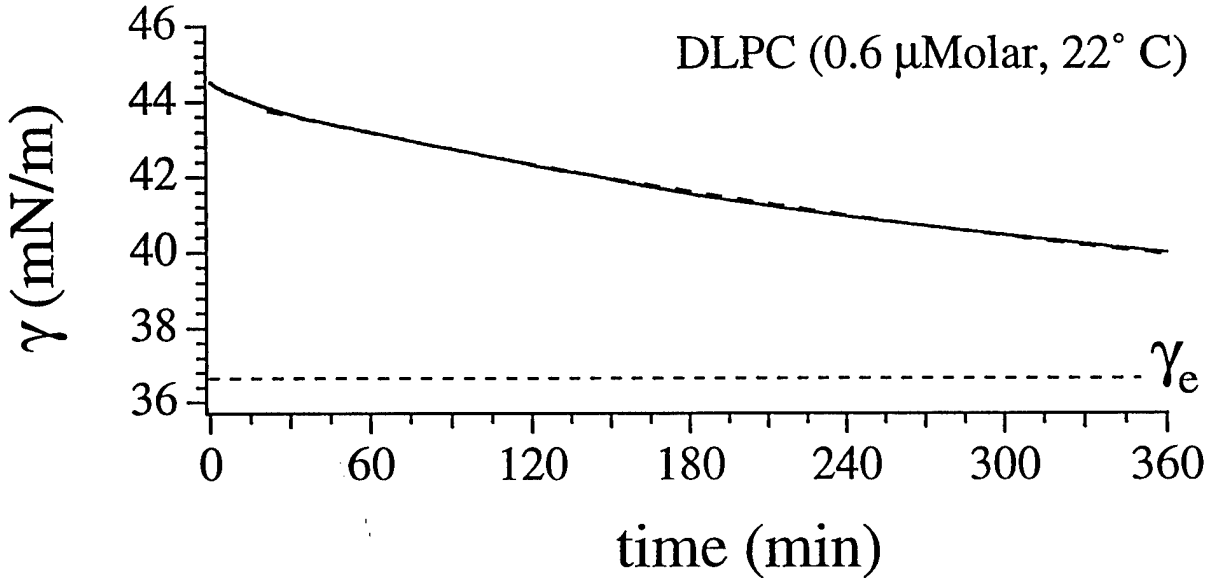

Walker and Richmond
Figure 5

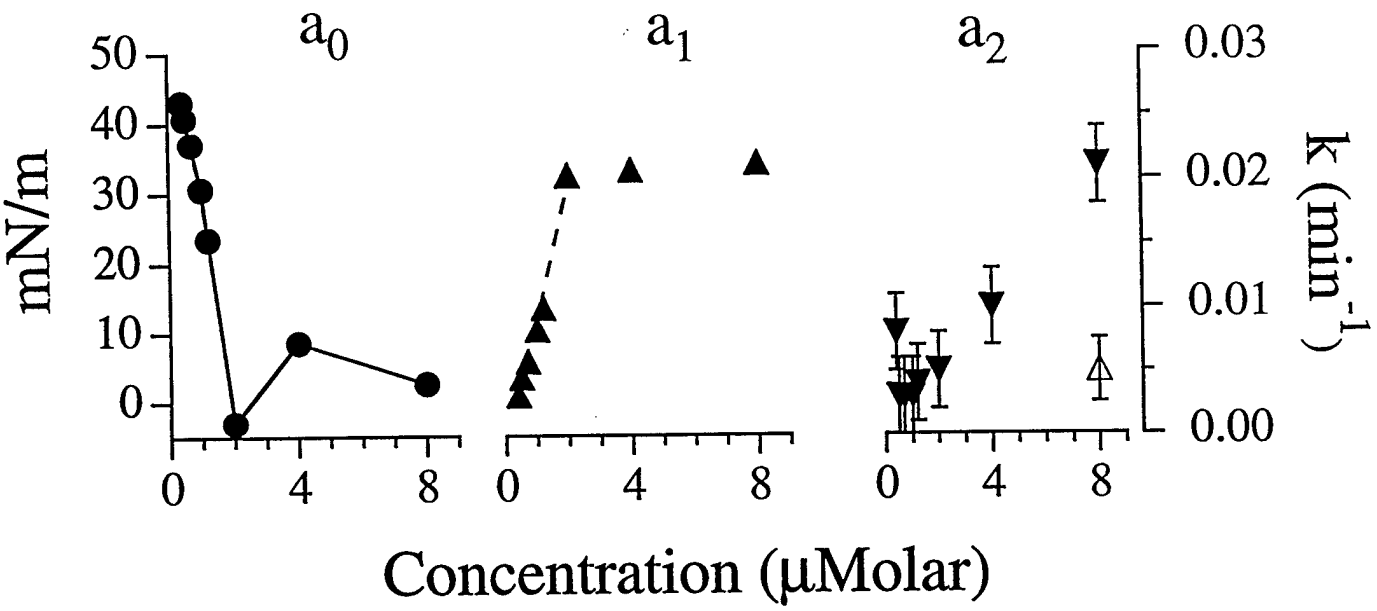

Walker and Richmond
Figure 6

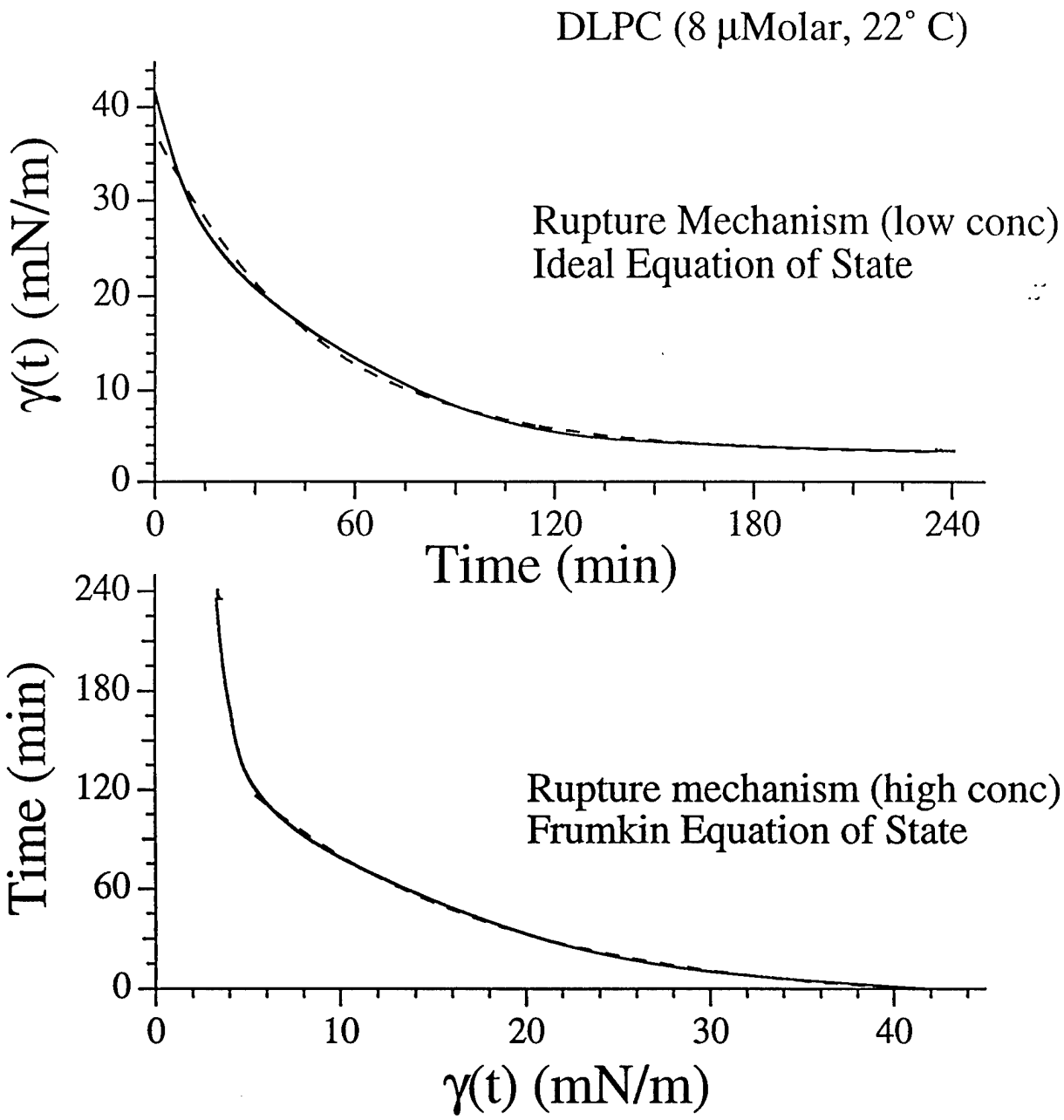

Walker and Richmond
Figure 7

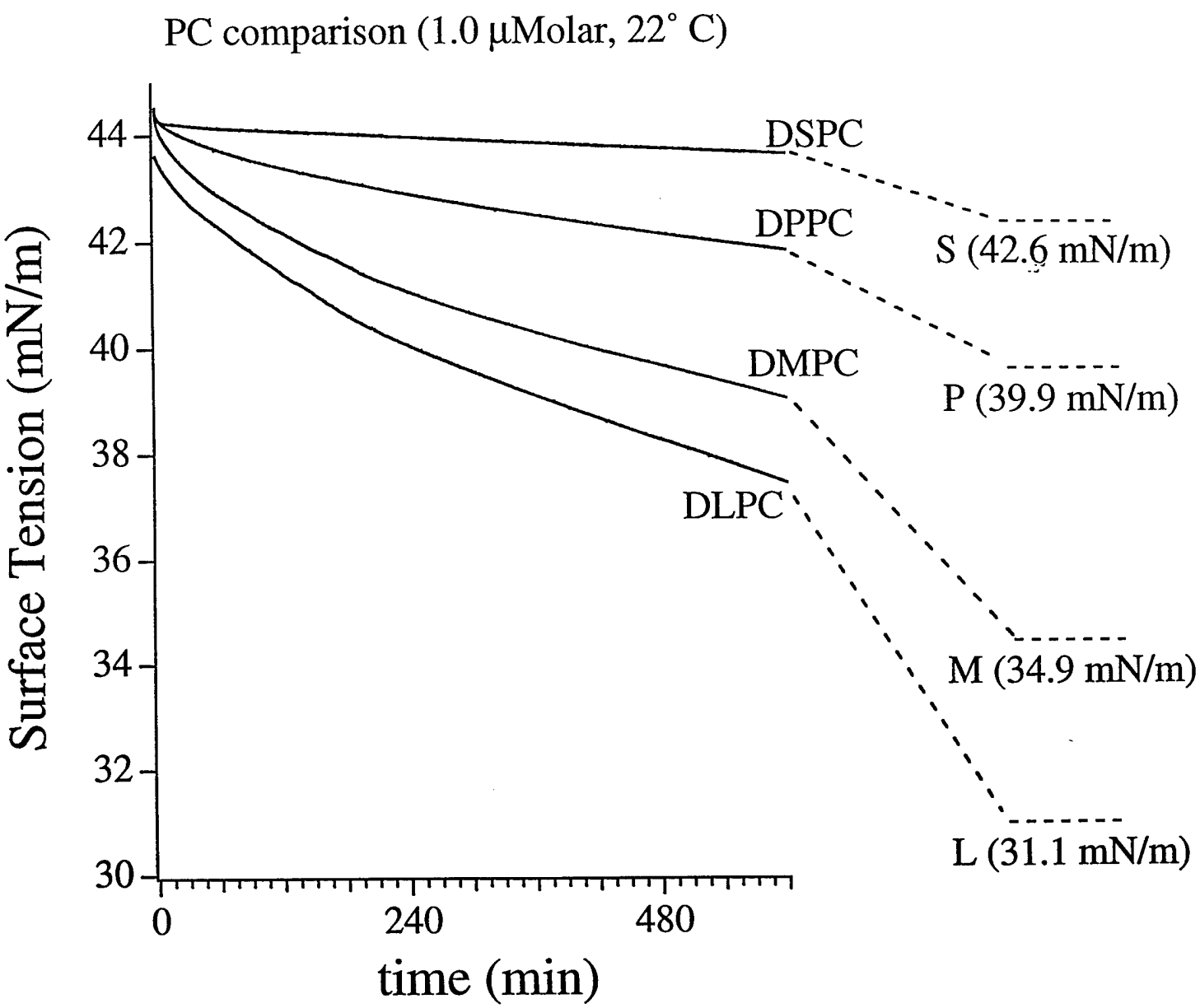

Walker and Richmond
Figure 8

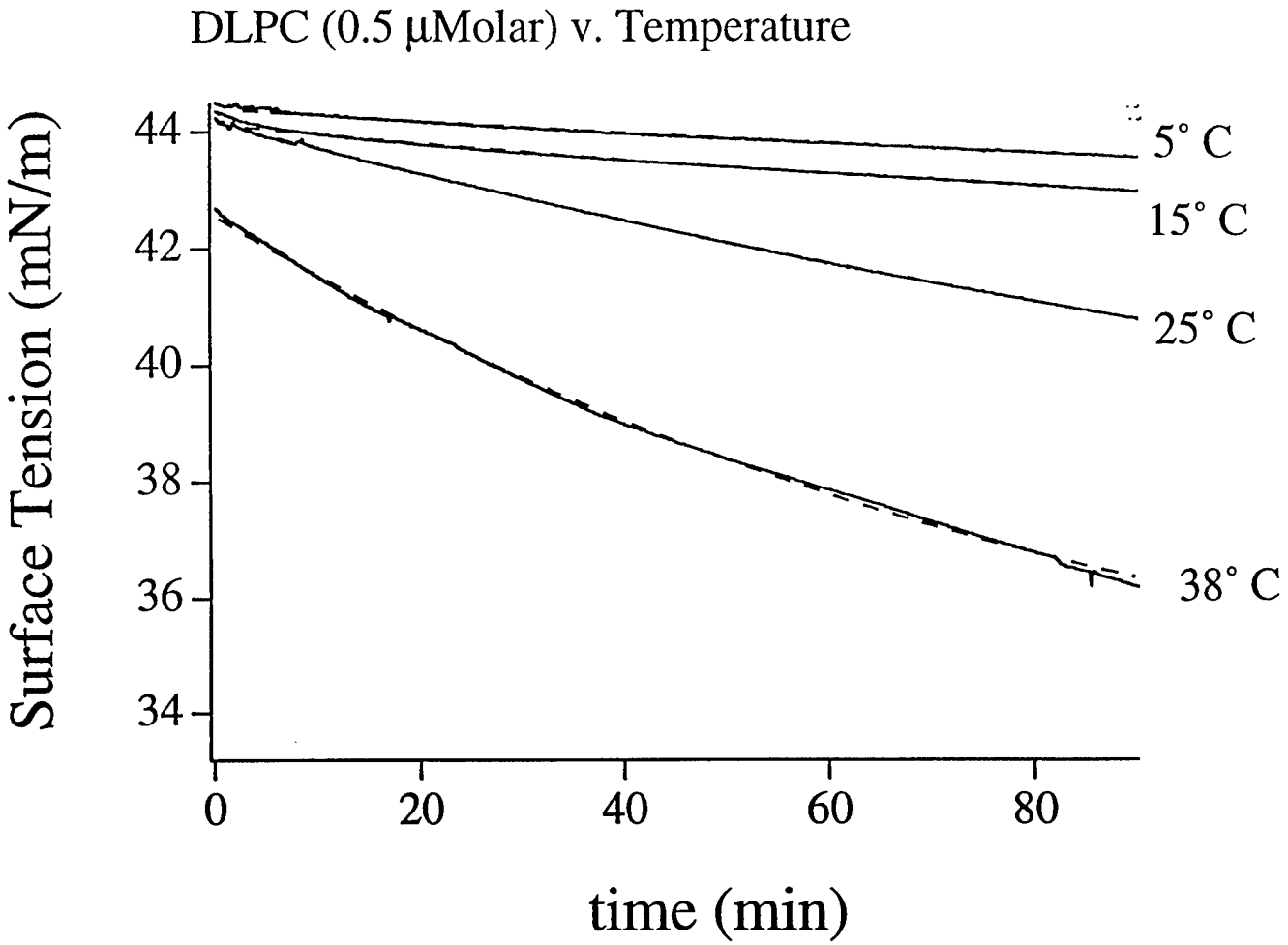

Walker and Richmond
Figure 9

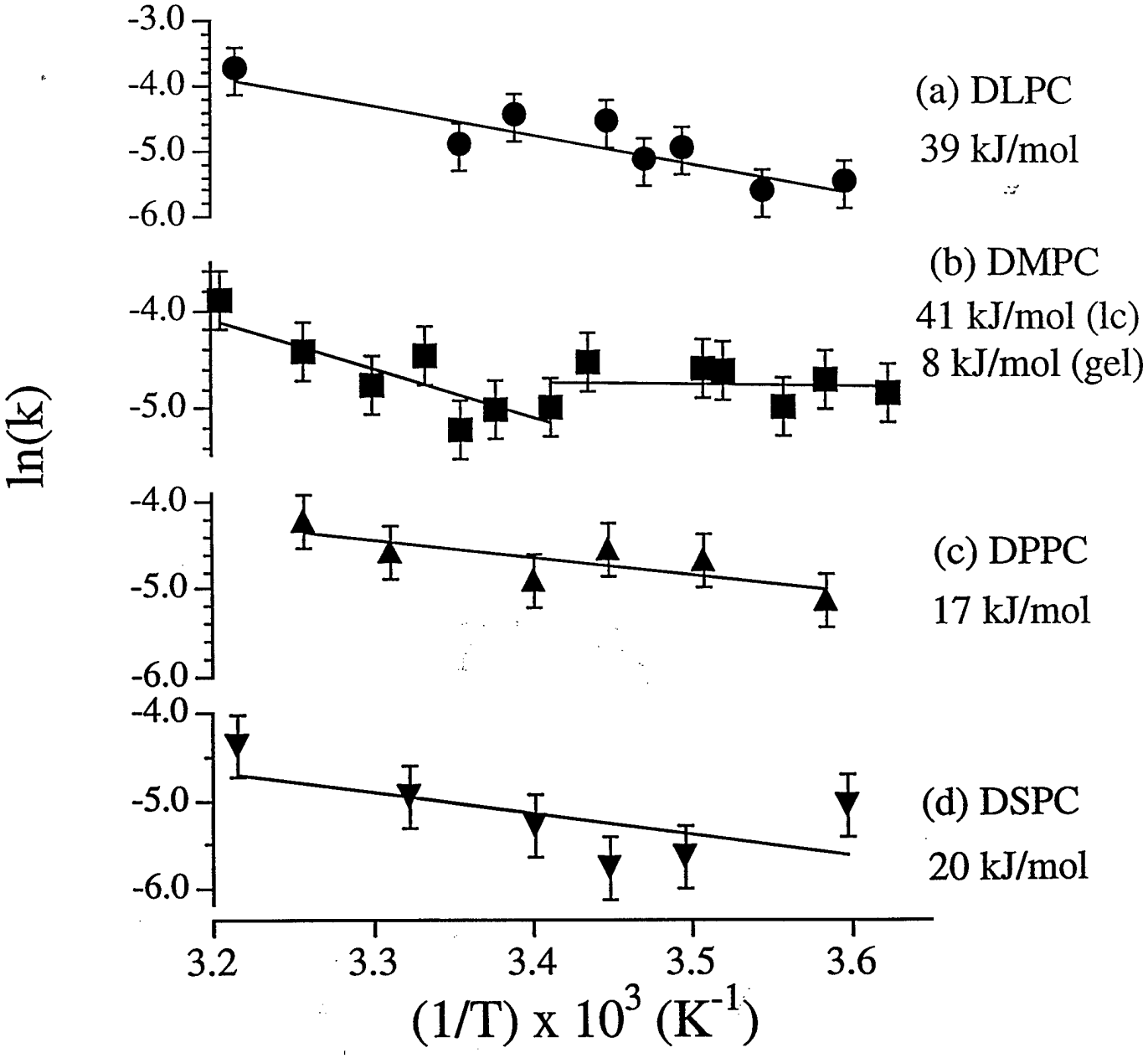

Walker and Richmond

Figure 10

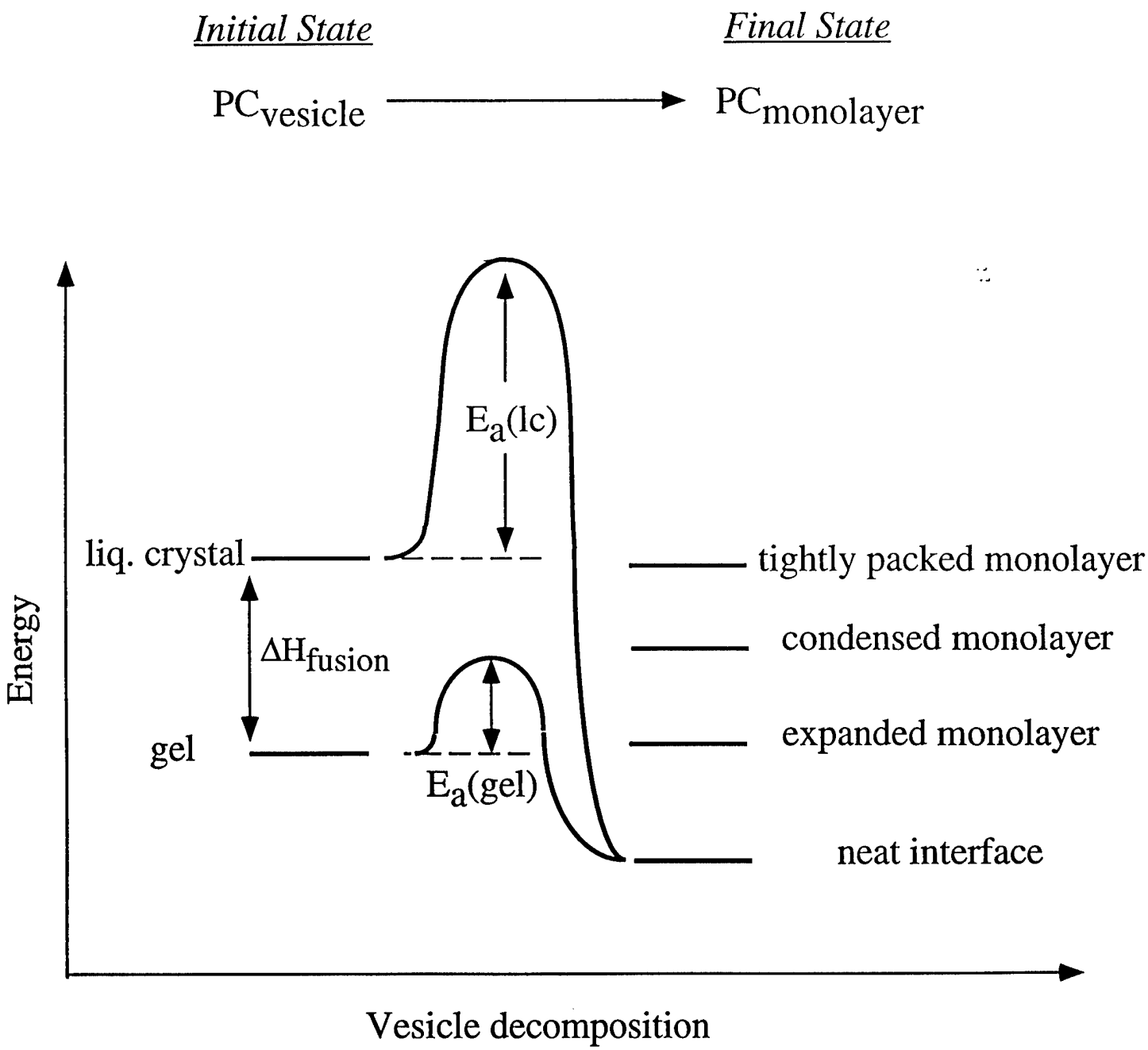

Walker and Richmond

Figure 11